Comparison of Fully-Differential and Single-Ended Current-Mode Band-Pass Filters with Current Active Elements

Jan Jerabek[1], Jaroslav Koton[1], Roman Sotner[2], and Kamil Vrba[1]

[1]Brno University of Technology, Faculty of Electrical Engineering and Communication, Department of Telecommunications, Purkynova 118, 612 00 Brno, Czech Republic
jerabekj@feec.vutbr.cz, koton@feec.vutbr.cz, vrbak@feec.vutbr.cz
[2]Brno University of Technology, Faculty of Electrical Engineering and Communication, Department of Radio Electronics, Purkynova 118, 612 00 Brno, Czech Republic
xsotne00@stud.feec.vutbr.cz

Abstract

Two single-ended (S-E) and two fully-differential (F-D) band-pass filters are shown and compared in this contribution. Filters contain only simple current followers with multiple outputs and one current amplifier with digitally adjustable gain that is used to control the quality factor of each filter with direct or inverse proportion. Simulation results are included, and the values of quality factor obtained for each of the solutions are assessed.

1. Introduction

F-D structures [1 – 8] bring several benefits compared to the single-ended (S-E) circuits, such as a greater dynamic range of the signal being processed, greater attenuation of common-mode signal, better power supply rejection ratio, and lower harmonic distortion. Unsurprisingly, F-D structures also have some drawbacks. These are, in particular, the large area taken up on the chip, related to greater power consumption, and sometimes the more complicated design.

The basics of the design of simple F-D structures with a high Common Mode Rejection Ratio (CMRR) with the help of coupling two S-E structures were described in [1]. Transconductance elements such as the Balanced Operational Transconductance Amplifier (BOTA) [2] are traditionally present in F-D filters. Differential-input buffered and transconductance amplifiers (DBTA) [3] can also be applied. The Fully Differential Current Feedback Operational Amplifier (FDCFOA) operating in the voltage mode and having various internal structures is quite common [4] such as fully-differential current conveyors of the second generation (FDCCII) [5 – 6] or fully-differential current followers (FD-CF) [8]. The structures often work in the voltage-mode (VM); however, current research in analog functional blocks is also focused on the realization of the current-mode (CM) filters. Various conceptions of simple F-D circuits suitable for the processing of current-mode signals can be found in [7].

The methodology for the F-D filter design with various target requirements for the designed filtering structures was presented in [9], for instance.

Recently, current followers with non-unity gain [10] or current amplifiers [11 – 12] were presented that might be suitable for high-frequency applications. In [8], [13 – 14], the digitally adjustable current amplifier (DACA) has been presented. It has differential current input and output, and the gain can be digitally controlled, as shown later in this contribution.

Our two structures of the band-pass F-D filter operate in the current mode and are compared with their S-E equivalents. Both provide the possibility of digital adjustment of the quality factor, which is beneficial. Simple multiple-output current followers (MO-CF) [15 – 16] and DACA are used as active elements. The design of these structures was performed by a simple transformation method, starting from the S-E circuits.

2. Active Elements

The S-E and F-D structures presented here operate with two types of active element. One is a simple current active element with dual or multiple outputs (DO-CF, MO-CF) [15]. As an example, the DO-CF schematic symbol is shown in Fig. 1(a), a 3rd-level simulation model suitable for AC analysis is shown in Fig. 1(b), and its outer behavior is described by

$$\boldsymbol{I}_{\mathrm{OUT+}} = -\boldsymbol{I}_{\mathrm{OUT-}} = \boldsymbol{I}_{\mathrm{IN}} \ . \qquad (1)$$

The MO-CF schematic symbol, simulation model and equations are easy to derive.

A Digitally Adjustable Current Amplifier (DACA) (Fig. 2a) is the other active element. DACA has adjustable current gain (A), which is controlled by three digital bits. The DACA circuit was lately developed in cooperation with ON Semiconductor inc. in the CMOS 0.35 μm technology. We have several samples

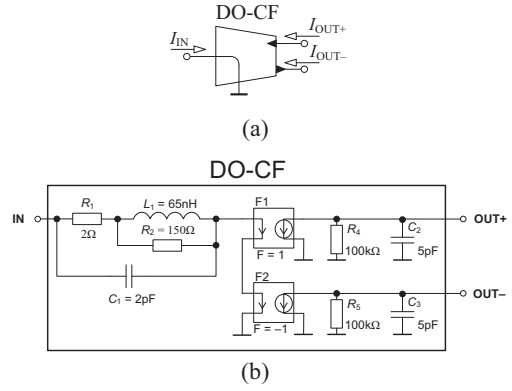

Fig. 1. Dual output Current Follower (DOCF): (a) schematic symbol, (b) 3rd order AC simulation model

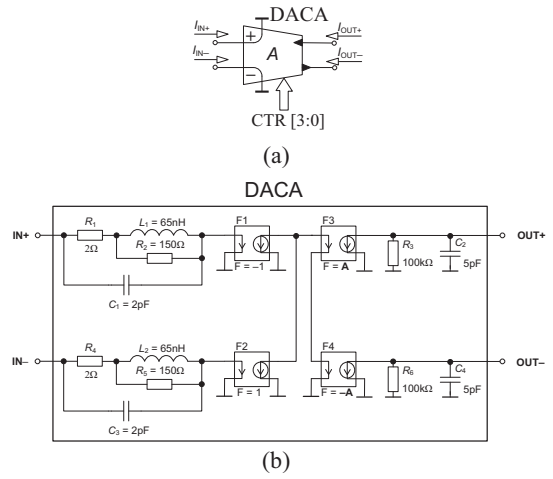

Fig. 2. Digitally Adjustable Current Amplifier (DACA): (a) schematic symbol, (b) 3rd-order AC simulation model

from the second test batch available and they are currently undergoing the first set of tests. The DACA 3rd-level AC simulation model is depicted in Fig. 2b. The current transfers of the DACA element are given by the relations

$$\boldsymbol{I}_{\mathrm{OUT+}} = A\,(\boldsymbol{I}_{\mathrm{IN+}} - \boldsymbol{I}_{\mathrm{IN-}}),\ \boldsymbol{I}_{\mathrm{OUT-}} = -A\,(\boldsymbol{I}_{\mathrm{IN+}} - \boldsymbol{I}_{\mathrm{IN-}})\,. \quad (2)$$

If input and output differential currents of DACA are defined by

$$\boldsymbol{I}_{\mathrm{ID}} = \boldsymbol{I}_{\mathrm{IN+}} - \boldsymbol{I}_{\mathrm{IN-}}\ ,\ \ \boldsymbol{I}_{\mathrm{OD}} = \boldsymbol{I}_{\mathrm{OUT+}} - \boldsymbol{I}_{\mathrm{OUT-}}\,, \quad (3)$$

then the differential current gain of the DACA element is given by

$$\boldsymbol{I}_{\mathrm{OD}} = 2\,A\,\boldsymbol{I}_{\mathrm{ID}}\,. \quad (4)$$

Measurement results for the DACA features are not yet available, therefore the DACA model is derived from the results of transistor-level simulation of the final DACA chip before production. The 3rd-order simulation model of the DO-CF was derived from the expected results of real DACA devices. It is obvious that these models do not cover all possible parameters of the above-mentioned active elements, but they are sufficient enough for an AC analysis and meaningful comparison of the solutions designed.

3. Proposed Frequency Filters

The DACA active element is suitable for the design of both the F-D and the S-E frequency filters working in the current mode. In Fig. 3, two circuit topologies of S-E band-pass filters are shown, Fig. 4 shows the signal-flow graphs of the circuits designed. By suitably interconnecting unity-gain dual- and multiple- output current followers (DO-CF, MO-CF) and using a single DACA, the quality factor Q can be adjusted independently of the natural frequency ω_0 and the pass-band gain. The current transfer function of the first variant (Fig. 3a) is

$$K_{1(S-E)} = -\frac{\boldsymbol{s}C_1R_1A}{\boldsymbol{s}^2C_1C_2R_1R_2 + \boldsymbol{s}C_1R_1A + 1}\,, \quad (5)$$

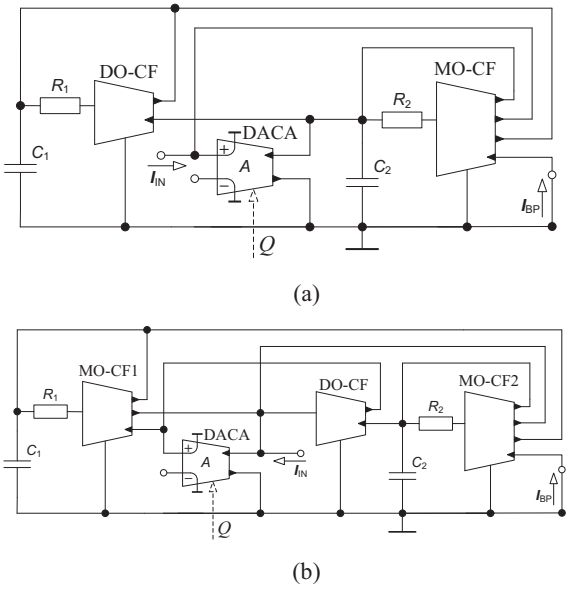

Fig. 3. Single-ended band-pass filter with current active elements and adjustable quality factor (a) first solution (Q controlled by A – inverse proportion) (b) second solution (Q controlled by A – direct proportion)

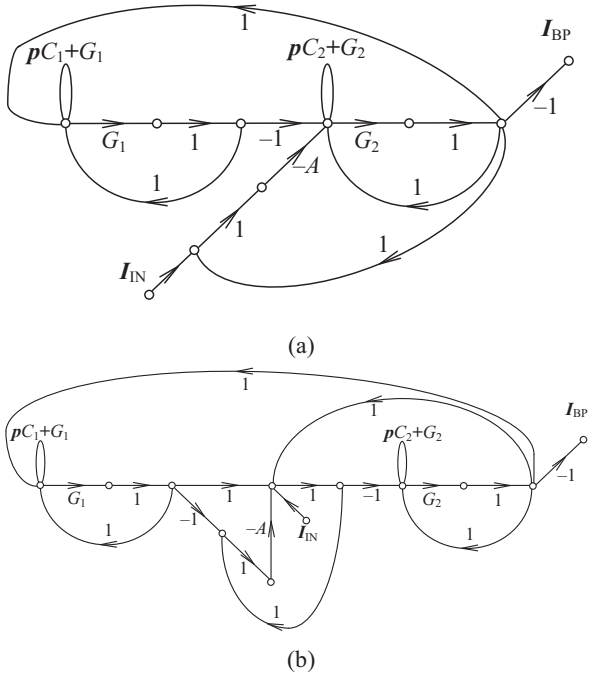

Fig. 4. Signal-flow graph of proposed band-pass filters (a) first solution (b) second solution

where the center frequency and the quality factor are expressed as

$$f_{0\_1(S\text{-}E)} = \frac{1}{2\pi}\sqrt{\frac{1}{R_1R_2C_1C_2}}\ ,\quad Q_{1(S\text{-}E)} = \frac{1}{A}\sqrt{\frac{R_2C_2}{R_1C_1}}\ . \quad (6)$$

The current transfer function of the second variant from Fig. 3b is

$$K_{2(S-E)} = -\frac{sC_1R_1}{s^2C_1C_2R_1R_2(1+A)+sC_1R_1A+(1+A)}, \quad (7)$$

where the center frequency and quality factor are expressed as

$$f_{0\_2(SE)} = \frac{1}{2\pi}\sqrt{\frac{1}{R_1R_2C_1C_2}}, \quad Q_{2(S-E)} = (1+A)\sqrt{\frac{R_2C_2}{R_1C_1}}. \quad (8)$$

The S-E filters presented were easily transformed into F-D filters shown in Fig. 5. The structures have the same features, but the transfer functions are changed because of the differential gain of DACA, which is twice higher (4). The current transfer function of the first variant from Fig. 5a is

$$K_{1(F-D)} = -\frac{sC_1R_1 2A}{s^2C_1C_2R_1R_2+sC_1R_1 2A+1}, \quad (9)$$

where the center frequency and the quality factor are

$$f_{0\_1(F\text{-}D)} = \frac{1}{2\pi}\sqrt{\frac{1}{R_1R_2C_1C_2}}, \quad Q_{1(F\text{-}D)} = \frac{1}{2A}\sqrt{\frac{R_2C_2}{R_1C_1}}. \quad (10)$$

The current transfer function of the second variant from Fig. 5b is

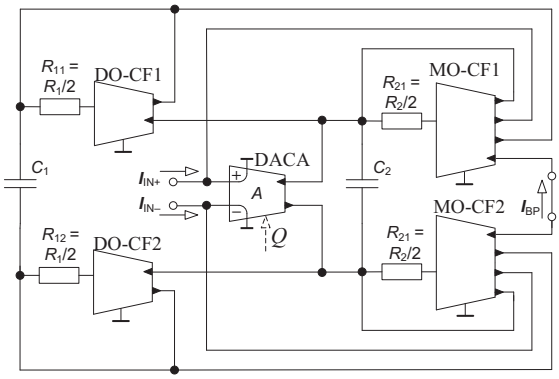

(a)

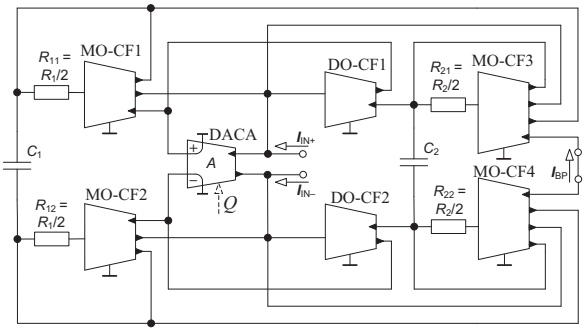

(b)

Fig. 5. Fully-differential band-pass filter with current active elements and adjustable quality factor (a) first solution (Q controlled by A – inverse proportion) (b) second solution (Q controlled by A – direct proportion)

$$K_{2(F-D)} = -\frac{sC_1R_1}{s^2C_1C_2R_1R_2(1+2A)+sC_1R_1A+(1+2A)}, \quad (11)$$

where the center frequency and the quality factor can be expressed as

$$f_{0\_2(F\text{-}D)} = \frac{1}{2\pi}\sqrt{\frac{1}{R_1R_2C_1C_2}}, \quad Q_{2(F\text{-}D)} = (1+2A)\sqrt{\frac{R_2C_2}{R_1C_1}}. \quad (12)$$

It is obvious that the quality factor of filters from Fig. 3a and Fig. 5a can be controlled by DACA gain A (inverse proportion) and, in the case of filters from Fig. 3b and Fig. 5b, also by DACA gain A (direct proportion).

4. Simulation results

To verify the theoretical presumptions, the behavior of all proposed filtering circuits has been analyzed by Spice simulations. The chosen or calculated values are summarized in Table 1. Center frequency is f_0 = 1 MHz in each case.

Simulation results comparing the S-E and the F-D filter are shown in Fig. 6a (first variant) and Fig. 6b (second variant). DACA gain A was adjusted to 1, 2, 4 and 8 in each case.

The obtained values of quality factor compared to the theoretical values are summarized in Table 2. It is obvious that the simulated values are lower than expected, especially when Q is high. Results for the F-D filters are closer to the theory. Because of the double differential gain of DACA element and because of the format of transfer function (9), the second F-D variant does not have the same range of quality factor adjustment as the S-E filter.

The second conception is more beneficial because its simulation results are closer to the theoretical assumptions (not shown in the graphs). Low-frequency attenuation is lower than expected (22-42 dB) in the first case. It is caused by the finite output impedance of the active elements used, which is expected to be only 100 kΩ at low frequencies, and in the case of the R_2 - C_2 node, where three output impedances are in parallel, it is actually only 33 kΩ. This impedance forms a significant current divider together with R_2 and therefore better attenuation cannot be achieved. The lower value of R_2 could be used if this structure is preferred and the low-frequency attenuation has to be improved. The second conception has only two output impedances in parallel in this R_2 - C_2 node and therefore its impedance is 50 kΩ, which significantly improves the low frequency results. It is clear that a higher number of active elements is beneficial in particular cases. High-frequency performance of both filters designed and in both S-E and F-D variants is very close to the theory. Naturally, when more complex models are used or active elements are replaced by transistor-level representation, we could expect more disturbed high frequency response. Nevertheless, these current-only active elements should provide better high-frequency performance than other kind of circuits.

Monte Carlo analysis was performed in order to show the dissipation of results and also to compare the S-E and F-D solution. Inner passive elements included in model of each of active elements were modeled with 10% tolerance in case of resistors and 20% tolerance in case of capacitors and inductors. Outside resistors and capacitors that are present in designed structures were modeled with 5% tolerance of resistors and 10% tolerance of capacitors. All filtering structures were simulated

with Gaussian distribution and two graphs are included in this contribution as an example of simulation results. First (Fig. 7a) shows results for first solution in S-E variant and for the highest quality factor and second (Fig. 7b) shows the F-D variant of the same filter. The difference between the lowest and the highest center frequency is 243 kHz in case of the S-E solution and 303 kHz in case of the F-D filter. Worse results of F-D variant are caused by uncorrelated tolerances of passive elements in simulation. If tolerances are correlated, which represents more realistic scenario, results of the F-D solution should be better than results of the S-E filter.

Table 1. Passive component values and range of quality factor adjustment by current gain of DACA element for each of presented band-pass filters

Variant	C_1 [pF]	C_2 [pF]	R_1 [Ω]	R_2 [Ω]	Q_{range} [-]
1 (S-E)	51	680	560	1300	0.7 – 5.6
1 (F-D)	39	1200	360	1500	0.7 – 5.6
2 (S-E)	410	47	1100	1200	0.7 – 3.1
2 (F-D)	410	44	1640	860	0.7 – 4.0

Table 2. Theoretical a simulated values of quality factor for different DACA gains and for all designed band-pass filters

	First solution (S-E)				First solution (F-D)			
A [-]	1	2	4	8	1	2	4	8
Q_{teor} [-]	5.6	2.8	1.4	0.7	5.6	2.8	1.4	0.7
Q_{sim} [-]	3.9	2.3	1.3	0.8	4.5	2.5	1.4	0.8
	Second solution (S-E)				Second solution (F-D)			
A [-]	1	2	4	8	1	2	4	8
Q_{teor} [-]	0.7	1.0	1.7	3.1	0.7	1.2	2.1	4.0
Q_{sim} [-]	0.9	1.2	1.8	2.8	0.9	1.3	2.1	3.7

5. Conclusions

Two fully-differential and two single-ended band-pass filters were shown in this contribution. Each structure includes only current active elements and is designed to work in the current mode. The quality factor is controlled digitally by the current gain of one DACA element (dependence of Q on A is direct or inverse), which is placed appropriately in each of the structures. The simulations of both the S-E and the F-D filter proved the design correctness and the possibility of quality factor adjustment.

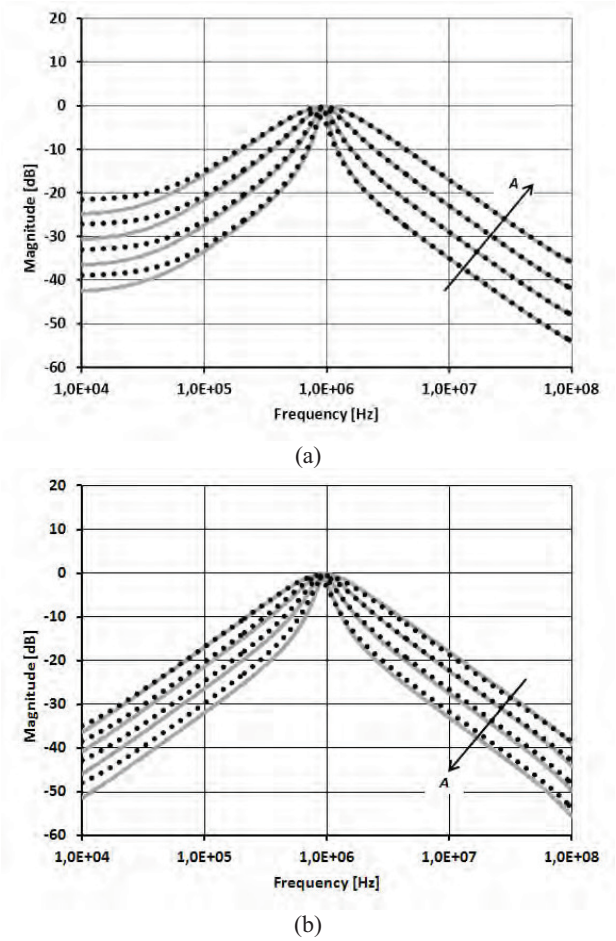

(a)

(b)

Fig. 6. Simulation results, comparison of S-E and F-D band-pass filter with Q adjustment (a) first solution (b) second solution
— F-D filter ••• S-E filter

It is obvious that all designed filters have acceptable and comparable magnitude responses. When the advantages of the F-D filter, which were mentioned in the introductory part, are considered together with the better quality factor values, the F-D filter is a better choice, especially when F-D signals are processed.

When the first and the second type of band-pass filter solutions are compared, the solution with the direct quality factor to gain proportion seems to have better properties, especially on low frequencies, as can be seen from the graphs.

6. Acknowledgment

The research described in this contribution was supported by Czech Science Foundation project No. 102/09/1681 and by the Czech Ministry of Education, program MSM 0021630513.

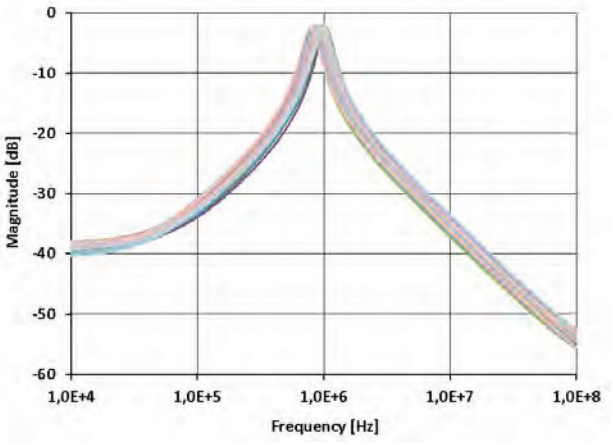

(a)

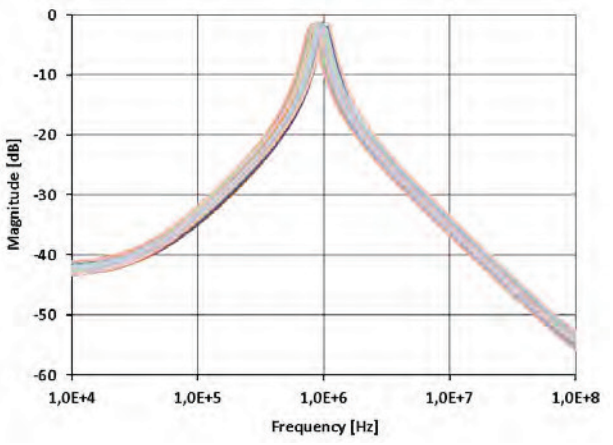

(b)

Fig. 7. Simulation results of the Monte Carlo analysis with Gaussian distribution; comparison of the first S-E and F-D band-pass filter with *Q* adjusted to the highest value (a) S-E filter (b) F-D filter

7. References

[1] O. Casas, R. Pallas-Areny, "Basics of Analog Differential Filters". *IEEE Transaction Instrumentation Measurement* Vol. 45, No. 1, pp. 275-279, 1996.

[2] M. O. Shaker, S. A. Mahmoud, A. M. Soliman, "New CMOS Fully-Differential Transconductor and Application to a Fully-Differential Gm-C Filter". *ETRI Journal*, Vol. 28, No. 2, 2006.

[3] N. Herencsár, J. Koton, K. Vrba, "Differential-Input Buffered and Transconductance Amplifier (DBTA)-Based New Trans-Admittance- and Voltage-Mode First-Order All- Pass Filters". *In Proceedings of the 6th International Conference on Electrical and Electronics Engineering - ELECO' 09*. Turkey: EMO Yayinlari, pp. 256-259, 2009.

[4] S. A. Mahmoud, "Low Voltage Fully Differential CMOS Current Feedback Operational Amplifier", *Proc 47th IEEE Midwest Int Symposium Circuits and Systems*, Vol. 1, pp. 49-52, 2004.

[5] E.A. Soliman, S.A. Mahmoud, "New CMOS fully differential current conveyor and its application in realizing sixth order complex filter". *IEEE International Symposium Circuits and Systems*, pp. 57-60, 2009.

[6] E.A. Sobhy, A.M. Soliman, "Realizations of fully differential voltage second generation current conveyor with an Application". *International Journal of Circuit Theory and Applications*, Vol. 38, No. 5, 2010.

[7] R.H. Zele, D.J. Allstot, T.S. Fiez, "Fully balanced CMOS current-mode circuits". *IEEE Journal of Solid-State Circuits*, Vol. 28, No. 5, pp. 569-575, 1993.

[8] J. Jerabek, R. Sotner, K. Vrba, "Fully-differential current amplifier and its application to universal and adjustable filter". *In 2010 Int Conf on Applied Electronics*. Pilsen: University of West Bohemia, Czech Republic, pp. 141-144, 2010.

[9] M. Massarotto, O. Casas, V. Ferrari, R. Pallas-Areny, "Improved Fully Differential Analog Filters". *IEEE Transaction on Instrumentation and Measurement*, Vol. 56, No. 6, pp. 2464-2469, 2007.

[10] W. Tangsrirat and T. Pukkalanun, "Digitally programmable current follower and its applications," *Int. J. Electron. Commun. (AEU)*, vol. 63, no. 5, pp. 416-422, 2009.

[11] H. A. Alzaher, "A CMOS digitally programmable universal current mode filter," *IEEE Trans. Circuits and Systems II*, vol. 55, no. 8, pp. 758-762, 2008.

[12] B. Sedighi and M. S. Bakhtiar, "Variable gain current mirror for highspeed appications," *IEICE Electronics Express*, vol. 4, no. 8, pp. 277-281, 2007.

[13] J. Koton, N. Herencsar, J. Jerabek, K. Vrba, "Fully Differential Current-Mode Band-Pass Filter: Two Design Solutions". *In Proc. 33rd Int Conf on Telecom and Signal Procesing, TSP 2010*. Baden, Austria, pp. 1-4, 2010.

[14] J. Jerabek, K. Vrba, M. Jelinek, "Universal Fully-Differential Adjustable Filter with Current Conveyors and Current Amplifier in Comparison with Single-Ended Solution," *In 2011 Int Conf on Applied Electronics*. Pilsen: University of West Bohemia, Czech Republic, pp.189-192, 2011.

[15] J. Jerabek, K. Vrba, "Design of SIMO- type Universal Filter with Adjustable Parameters". *In Proceedings of the 32nd International Conference on Telecommunications and Signal Processing - TSP' 2009*. Budapest: Hungary, pp. 38-42, 2009.

[16] J. Jerabek, K. Vrba, „Design of Fully-Differential Filters with nth-order Synthetic Elements and Comparison with Single- Ended Solution". In Proc of the 2011 Int Conf on Computer and Communication Devices (ICCCD 2011). Bali, Indonesia, pp. V1- 48 – V1-52, 2011.